

# Topological Equivariant Artist Model

Hannah Aizenman, Thomas Caswell, Michael Grossberg

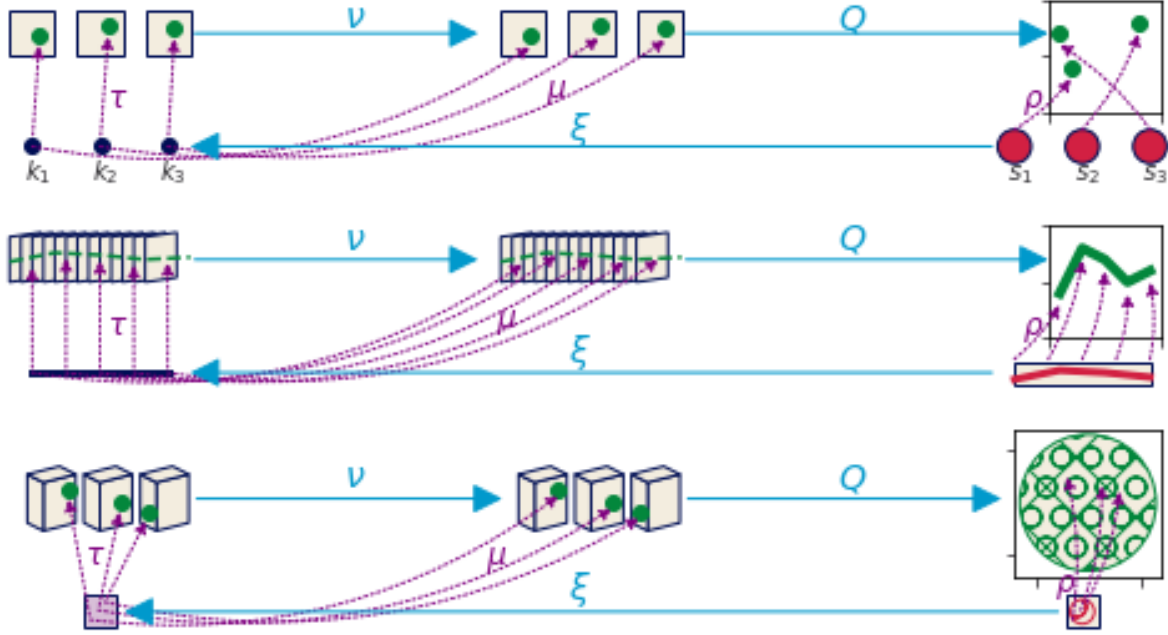


Fig. 1: Visualizations consist of topologically equivariant maps. There is a set of monoid action equivariant maps from data components to visual components  $v$  that are then reduced via  $Q$  into a single graphic, and there is a deformation retraction  $\xi$  from graphic continuity to data continuity.

**Abstract**—This work presents a functional model of the structure-preserving maps from data to visual representation to guide the development of visualization libraries. Our model, which we call the topological equivariant artist model (TEAM), provides a means to express the constraints of preserving the data continuity in the graphic and faithfully translating the properties of the data variables into visual variables. We formalize these transformations as actions on sections of topological fiber bundles, which are mathematical structures that allow us to encode continuity as a base space, variable properties as a fiber space, and data as binding maps, called sections, between the base and fiber spaces. This abstraction allows us to generalize to any type of data structure, rather than assuming, for example, that the data is a relational table, image, data cube, or network-graph. Moreover, we extend the fiber bundle abstraction to the graphic objects that the data is mapped to. By doing so, we can track the preservation of data continuity in terms of continuous maps from the base space of the data bundle to the base space of the graphic bundle. Equivariant maps on the fiber spaces preserve the structure of the variables; this structure can be represented in terms of monoid actions, which are a generalization of the mathematical structure of Stevens' theory of measurement scales. We briefly sketch that these transformations have an algebraic structure which lets us build complex components for visualization from simple ones. We demonstrate the utility of this model through case studies of a scatter plot, line plot, and image. To demonstrate the feasibility of the model, we implement a prototype of a scatter and line plot in the context of the Matplotlib Python visualization library. We propose that the functional architecture derived from a TEAM based design specification can provide a basis for a more consistent API and better modularity, extendability, scaling and support for concurrency

**Index Terms**—Taxonomy, Models, Frameworks, Theory

## 1 INTRODUCTION

- Hannah Aizenman and Michael Grossberg are with the Computer Science department, City College of New York. E-mail: haizenman@ccny.cuny.edu, mgrossberg@ccny.cuny.edu.
- Thomas Caswell is with National Synchrotron Light Source II, Brookhaven National Lab E-mail: tcaswell@bnl.gov.

Manuscript received xx xxx. 201x; accepted xx xxx. 201x. Date of Publication xx xxx. 201x; date of current version xx xxx. 201x. For information on obtaining reprints of this article, please send e-mail to: reprints@ieee.org. Digital Object Identifier: xx.xxxx/TVCG.201x.xxxxxxx

The underlying structure and semantics of visualization are by definition reflected in visual representations [30], whether through direct mappings from data into visual elements or via figurative representations that have meaning due to their similarity to external concepts [21]. Visualization tools allow practitioners to automate these transformations, but most visualization tools are either explicitly tuned to specific continuity [40] or define every interface relative to its expected data structure. The former

1  
2  
3  
4  
5  
6  
7  
8  
9

approach is often too restrictive for a general purpose tool, while the latter often results in a library that can feel inconsistent or disjointed. Motivated by the challenge of rearchitecturing a general purpose visualization library, we developed the Topological Equivariant Artist Model (TEAM) to express the constraints of preserving data continuity and translating data properties into a visual representation. The contribution of TEAM is

1. topology preserving relationship between data and graphic via continuous maps
2. property preservation from data component to visual representation as equivariant maps that carry a homomorphism of monoid actions
3. functional oriented visualization tool architecture built on the mathematical model to demonstrate the utility of the model
4. prototype of the architecture built on Matplotlib’s infrastructure to demonstrate the feasibility of the model.

## 2 RELATED WORK

The components of a visual representation were first codified by Bertin [14], and the notion that the properties of the data and visual representation match is the basis of most evaluations of visualization. Expressiveness, as defined by Mackinlay [47, 48] is a measure of how much of the structure any map can encode. A fully expressive component is one that is equivariant since it has preserved all the structure in the data. Models of visualization evaluate this equivariance and how elements built in the model can be composed to build more complex visualizations. Mackinlay’s *A Presentation Tool* (APT) introduced the notion of visualizations having syntax and semantics [47] and Wilkenson described the grammar of this language [73]. This grammar oriented approach allows users to describe how to compose visual elements into a graphical design [75], while we are proposing a framework for building those elements. This same limitation is explicitly stated in the functional dependency model of visualization developed by Sugibuchi [67] and evident in Vickers’ category theory oriented framework in which semiotics are commutative. The algebraic process model by Kindlmann and Scheidegger proposes that the data and visualization transformations are commutative; while similar to our framework, it is missing any explicit mention of continuity.

Much of visualization algorithm design is oriented around continuity, as described in Tory and Möller’s taxonomy [68]. For example, the relational database is core to tools influenced by APT, such as Tableau [37, 49, 65] and the Grammar of Graphics [73] inspired ggplot [71], Vega [57] and Altair [70]. Images underpin scientific visualization tools such as Napari [59] and ImageJ [58] and the digital humanities oriented ImagePlot [66] macro; the need to visualize and manipulate graphs has spawned tools like Gephi [11], Graphviz [28], and Networkx [36]. Neither the table nor image nor graph model on its own supports all the data types a typical general purpose visualization library needs to support; instead libraries such as Matplotlib [43] and Vtk [32, 39] and D3 [16] explicitly carry around different data representations for all the different types of visualizations they support. Where libraries with a single core data structure have very consistent APIs, VTK, D3 and Matplotlib APIs can be rather inconsistent as every visualization has a different notion of how the data is structured.

Fiber bundle and sheafs are generalized abstractions proposed by Butler to encode the continuity of the data separately from the properties of each variable [19, 20]. Since Butler’s model lacks a robust way of describing variables, we fold in Spivak’s Simplicial formulation of databases [61, 62] to incorporate a schema like description of the variables. One way of describing the binding between the scheme and the continuity is using the notion of

structural *keys* with associated *values* proposed by Munzner [51]. Unlike Munzner’s model where the semantic meaning of the key is tightly coupled to the index of the value, our model considers keys to be a reference to topology. This allows the metadata to be altered, for example by changing the coordinate system or time resolution, without imposing new semantics on the underlying structure.

## 3 TOPOLOGICAL EQUIVARIANT ARTIST MODEL

We introduce the notion of an artist  $\mathcal{A}$  as an equivariant map

$$\mathcal{A} : \mathcal{E} \rightarrow \mathcal{H} \quad (1)$$

from data  $\mathcal{E}$  to graphic  $\mathcal{H}$ . To formalize the structure the artist is preserving, we describe how we model data (Sect. 3.1) and graphics (Sect. 3.2) as fiber bundles. We then discuss the equivariant maps that make up  $\mathcal{A}$ , which are a map from graphic continuity to data continuity (Sect. 3.2.1), data components to visual components (Sect. 3.3.1) and visual components to graphic (Sect. 3.3.2).

### 3.1 Data Bundle

Building on Butler’s proposal of using fiber bundles as a common data representation structure for visualization data [19, 20], a fiber bundle is a tuple  $(E, K, \pi, F)$  defined by the projection map  $\pi$

$$F \hookrightarrow E \xrightarrow{\pi} K \quad (2)$$

that binds the components of the data in  $F$  to the continuity represented in  $K$ . By definition fiber bundles are locally trivial [2, 60], meaning that over a localized neighborhood  $U$  the total space is the cartesian product  $K \times F$ .

#### 3.1.1 Fiber Space: Variables

To formalize the structure of the data components, we use notation introduced by Spivak [61] that binds the components of the fiber to variable names. Spivak constructs a set  $\mathbb{U}$  that is the disjoint union of all possible objects of types  $\{T_0, \dots, T_m\} \in \mathbf{DT}$ , where  $\mathbf{DT}$  are the data types of the variables in the dataset. He then defines the single variable set  $\mathbb{U}_\sigma$

$$\begin{array}{ccc} \mathbb{U}_\sigma & \longrightarrow & \mathbb{U} \\ \pi_\sigma \downarrow & & \downarrow \pi \\ C & \xrightarrow{\sigma} & \mathbf{DT} \end{array} \quad (3)$$

which is  $\mathbb{U}$  restricted to objects of type  $T$  bound to variable name  $c$ . The  $\mathbb{U}_\sigma$  lookup is by name to specify that every component is distinct, since multiple components can have the same type  $T$ . Given  $\sigma$ , the fiber for a one variable dataset is

$$F = \mathbb{U}_{\sigma(c)} = \mathbb{U}_T \quad (4)$$

where  $\sigma$  is the schema binding variable name  $c$  to its datatype  $T$ . A dataset with multiple variables has a fiber that is the cartesian cross product of  $\mathbb{U}_\sigma$  applied to all the columns:

$$F = \mathbb{U}_{\sigma(c_1)} \times \dots \times \mathbb{U}_{\sigma(c_i)} \times \dots \times \mathbb{U}_{\sigma(c_n)} \quad (5)$$

which is equivalent to

$$F = F_0 \times \dots \times F_i \times \dots \times F_n \quad (6)$$

which allows us to decouple  $F$  into components  $F_i$ . Each component of  $F$  is a dimension of the topological fiber space and is specified by a tuple of the form  $(c, T, \mathbb{U}_{\sigma(c)})$ . In Fig. 2 the plane fiber has components (*time*, *datetime*,  $\mathbb{R}$ ) and (*temperature*, *float*,  $\mathbb{R}$ ), while the cube fiber has components (*time*, *datetime*,  $\mathbb{R}$ ) and (*wind*, *wind*,  $\mathbb{R}^+ \times \mathbb{R}$ ) which encodes (*speed*, *direction*).

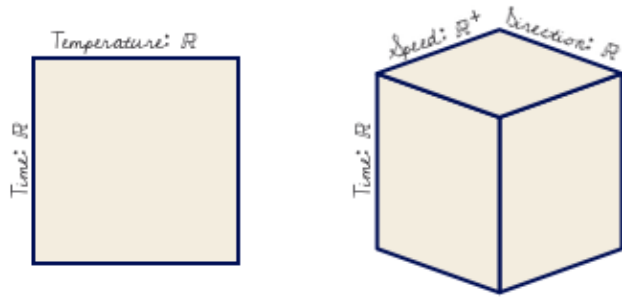


Fig. 2: These two datasets have the same base space  $K$ . The plane is a representation of the fiber  $F = \mathbb{R} \times \mathbb{R}$  for the variables (time, temperature), while the cube is the fiber  $\mathbb{R} \times \mathbb{R}^+ \times \mathbb{R}$  associated with (time, wind=(speed, direction))

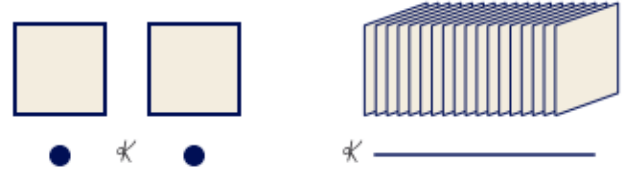


Fig. 3: These two datasets have the same fiber space  $F = \mathbb{R} \times \mathbb{R}$ , but the left dataset has a discrete continuity while the right is 1D continuous over the interval  $[0, 1]$ .

### 3.1.2 Equivariant Variable Properties: Monoid Actions

While structure on a set of values is often described algebraically as operations or through the actions of a group, for example Steven's measurement scales [45, 63], we generalize to monoids to support partial orderings. A partial ordering allows for multiple measurement values to have the same rank [29], which is useful for visualizing many types of multi indicator systems [17].

A monoid [7]  $M$  is a set with an associative binary operator  $*$ :  $M \times M \rightarrow M$ . A monoid has an identity element  $e \in M$  such that  $e * a = a * e = a$  for all  $a \in M$ . As defined on a component of  $F$ , a left monoid action [8, 54] of  $M_i$  is a set  $F_i$  with an action  $\bullet$ :  $M \times F_i \rightarrow F_i$  with the properties:

**associativity** for all  $f, g \in M_i$  and  $x \in F_i$ ,  $f \bullet (g \bullet x) = (f * g) \bullet x$

**identity** for all  $x \in F_i$ ,  $e \bullet x = x$

As with the fiber  $F$  the total monoid space  $M$  is the cartesian product

$$M = M_0 \times \dots \times M_i \times \dots \times M_n \quad (7)$$

of each monoid  $M_i$  on  $F_i$ . The monoid is also added to the specification of the fiber  $(c_i, T_i, \mathbb{U}_\sigma M_i)$

Defining the monoid actions on the components serves as the basis for identifying the invariance [44] that must be preserved in the visual representation of the component. A secondary advantage of defining structure in terms of monoids is that they are commonly found in functional programming because they specify compositions of transformations [64, 76].

### 3.1.3 Base Space: Continuity

The base space  $K$  acts as an indexing space, as emphasized by Butler [19, 20], to express how the records in  $E$  are connected to each other and does not itself store any of the components of the data. For example,  $K$  can encode that the timeseries data described in Sect. 3.1.1 is continuous, but is doing so independent of the timestamps. Every  $k \in K$  has a corresponding fiber  $F_k$  because  $K$  is the quotient space [5, 10] of  $E$ .

As illustrated in Fig. 3,  $K$  can have any number of dimensions, can be continuous or discrete, and is somewhat independent of the dimensions of the fiber. As with Equation 6 and Equation 7, we can decompose the total space into component bundles

$$\pi: E_1 \oplus \dots \oplus E_i \oplus \dots \oplus E_n \rightarrow K \quad (8)$$

such that  $M_i$  acts on component bundle  $E_i$ . The  $K$  remains the same because the connectivity of records does not change just because there are fewer components in each record. By encoding this continuity in the model as  $K$  the data model now explicitly carries information about its structure such that the implicit assumptions of the visualization algorithms are now

explicit. The explicit topology is a concise way of distinguishing visualizations that appear identical, for example heatmaps and images.

### 3.1.4 Section: Values

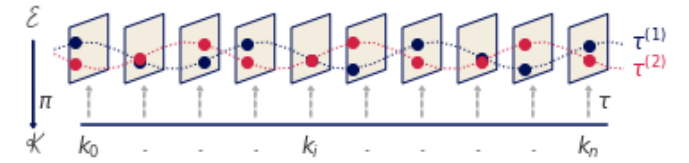


Fig. 4: Each section in the fiber bundle is a unique continuous map from base space to fiber encoding the set of records in the dataset. The two sections,  $\tau^{(1)}$  and  $\tau^{(2)}$ , shown here are in the set of global sections  $\Gamma(E)$ .

While the projection function  $\pi: E \rightarrow K$  ties together the base space  $K$  with the fiber  $F$ , a section  $\tau: K \rightarrow E$  encodes a dataset. A section function takes as input location  $k \in K$  and returns a record  $r \in E$ . For any fiber bundle, there exists a map

$$\begin{array}{ccc} F & \hookrightarrow & E \\ & \pi \downarrow & \uparrow \tau \\ & K & \end{array} \quad (9)$$

such that  $\pi(\tau(k)) = k$ . The set of all global sections is denoted as  $\Gamma(E)$ . As illustrated in Fig. 4, the section is a continuous mapping from a location  $k \in K$  on the base space to a record  $r \in F$  in the fiber. Assuming a trivial fiber bundle  $E = K \times F$ , the section is

$$\tau(k) = (k, (g_{F_0}(k), \dots, g_{F_n}(k))) \quad (10)$$

where  $g: K \rightarrow F$  is the index function into the fiber component. This formulation of the section also holds on locally trivial sections of a non-trivial fiber bundle. As with Equation 6 and Equation 8,  $\tau$  can be decomposed into components

$$\tau = (\tau_0, \dots, \tau_i, \dots, \tau_n) \quad (11)$$

where each section  $\tau_i$  maps into a record on a component  $F_i \in F$ . This allows for accessing the data component wise in addition to accessing the data in terms of its location over  $K$ .

### 3.1.5 Sheafs

A sheaf is a mathematical structure for defining collections of objects [33, 34, 69] on mathematical spaces. On the fiber bundle  $E$ , we can describe a sheaf as the collection of local sections  $\iota^* \tau$

$$\begin{array}{ccc} \iota^* E & \xleftarrow{\iota^*} & E \\ \pi \downarrow & \iota^* \tau & \pi \downarrow \tau \\ U & \xleftarrow{\iota} & K \end{array} \quad (12)$$

which are sections of  $E$  pulled back over local neighborhood  $U \subset E$  via the inclusion map  $\iota : E \rightarrow U$ . The bookkeeping enabled by sheafs is necessary for navigation techniques such as pan and zoom [53] and dynamically updated visualizations such as sliding windows [26,27]

### 3.2 Graphic Bundle

We introduce a graphic bundle to hold the essential information necessary to render a graphical design constructed by the artist. As with the data, we can represent the target graphic as a section  $\rho$  of a bundle  $(H, S, \pi, D)$

$$\begin{array}{ccc} D & \hookrightarrow & H \\ & \pi \downarrow \wr & \\ & S & \end{array} \quad (13)$$

where  $\rho$  is a fully specified graphic such that it is an abstraction of rendering. To fully specify the visual characteristics of the image, we construct a fiber  $D$  that is an infinite resolution version of the target space. Typically  $H$  is trivial and therefore sections can be thought of as mappings into  $D$ . In this work, we assume a 2D opaque image  $D = \mathbb{R}^5$  with elements  $(x, y, r, g, b) \in D$  such that a rendered graphic only consists of 2D position and color. By abstracting the target display space as  $D$ , the model can support different targets, such as a 2D screen or 3D printer.

#### 3.2.1 Equivariant Topology: Graphic Base Space

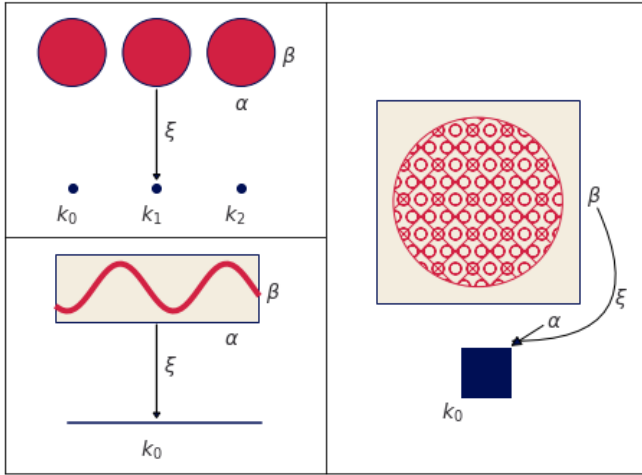


Fig. 5: The 0D scatter  $k$  and 1D line  $k$  are thickened into  $S$  with coordinates  $s = (\alpha, \beta)$  that are a region in an idealized 2D screen. The image has the same dimension in  $S$  as in  $K$ .

Just as the  $K$  encodes the connectivity of the records in the data, we propose an equivalent  $S$  that encodes the connectivity of the rendered elements of the graphic. Formally, we require that  $K$  be a deformation retract [6] of  $S$  so that  $K$  and  $S$  have the same homotopy. The surjective map  $\xi : S \rightarrow K$

$$\begin{array}{ccc} E & & H \\ \pi \downarrow & & \pi \downarrow \\ K & \xleftarrow{\xi} & S \end{array} \quad (14)$$

goes from region  $s \in S_K$  to its associated point  $s$ . While  $S$  must have the same continuity as  $K$  it is sometimes the thickened version shown in Fig. 5. This thickening is necessary when the dimensionality of  $K$  is less than the dimensionality of the target display. For example, a  $k$  that is 0D in  $K$  cannot be represented

on screen unless it is thickened to 2D to encode the connectivity of the points in  $D$  that visually represent the record at  $k$ . The  $\xi$  mapping is critical to interactive visualizations as it is the map from a region on screen to the data associated with that region. One example is to fill in details in a hover tooltip, another is to convert region selection on  $S$  to a query on the data to access the corresponding record components on  $K$ .

### 3.3 Artist

The topological artist  $A$  is a map from the sheaf on a data bundle  $E$  which is  $\mathcal{O}(E)$  to the sheaf on the graphic bundle  $H$ ,  $\mathcal{O}(H)$ .

$$A : \mathcal{O}(E) \rightarrow \mathcal{O}(H) \quad (15)$$

that carries a homomorphism of monoid actions  $\varphi : M \rightarrow M'$  [25]. Given  $M$  on data  $\mathcal{E}$  and  $M'$  on graphic  $\mathcal{H}$ , we propose that artists  $\mathcal{A}$  are equivariant maps

$$A(m \cdot r) = \varphi(m) \cdot A(r) \quad (16)$$

such that applying a monoid action  $m \in M$  to the data  $r \in \mathcal{E}$  input to  $\mathcal{A}$  is equivalent to applying a monoid action  $\varphi(m) \in M'$  to the graphic  $A(r) \in \mathcal{H}$  output of the artist.

The monoid equivariant map has two stages: the encoders  $\nu : E' \rightarrow V$  convert the data components to visual components, and the assembly function  $Q : \xi^*V \rightarrow H$  composites the fiber components of  $\xi^*V$  into a graphic in  $H$ .

$$\begin{array}{ccccc} E & \xrightarrow{\nu} & V & \xleftarrow{\xi^*} & \xi^*V & \xrightarrow{Q} & H \\ & \searrow \pi & \downarrow \pi & \swarrow \xi^* \pi & \downarrow \pi & \swarrow \pi & \\ & & K & \xleftarrow{\xi} & S & & \end{array} \quad (17)$$

$\xi^*V$  is the visual bundle  $V$  pulled back over  $S$  via the equivariant continuity map  $\xi : S \rightarrow K$  introduced in Sect. 3.2.1. The visual bundle  $(V, K, \pi, P)$  is the latent space of possible parameters of a visualization type, such as a scatter or line plot. As with the data and graphic bundles, the visual bundle is defined by the projection map  $\pi$

$$\begin{array}{ccc} P & \hookrightarrow & V \\ & \pi \downarrow \wr & \\ & K & \end{array} \quad (18)$$

where  $\mu$  is the visual variable encoding [14] of the data section  $\tau$ . The visual fiber  $P$  is defined in terms of the input parameters of the visualization library's plotting functions; by making these parameters explicit components of the fiber, we can build consistent definitions and expectations of how these parameters behave. The functional decomposition of the visualization artist facilitates building reusable components at each stage of the transformation because the equivariance constraints are defined on  $\nu$ ,  $Q$ , and  $\xi$ . We name this map the artist as that is the analogous part of the Matplotlib [42] architecture that builds visual elements.

#### 3.3.1 Visual Component Maps

We define the visual transformers  $\nu$

$$\{\nu_0, \dots, \nu_n\} : \{\tau_0, \dots, \tau_n\} \mapsto \{\mu_0, \dots, \mu_n\} \quad (19)$$

as the set of equivariant maps  $\nu_i : \tau_i \mapsto \mu_i$ . Given  $M_i$  is the monoid action on  $E_i$  and that there is a monoid  $M_i'$  on  $V_i$ , then there is a monoid homomorphism from  $\varphi : M_i \rightarrow M_i'$  that  $\nu$  must preserve. As mentioned in Sect. 3.1.2, monoid actions define the structure on the fiber components and are therefore the basis for equivariance. A validly constructed  $\nu$  is one where the diagram of the monoid transform  $m$  commutes

$$\begin{array}{ccc} E_i & \xrightarrow{\nu_i} & V_i \\ m_r \downarrow & & \downarrow m_v \\ E_i & \xrightarrow{\nu_i} & V_i \end{array} \quad (20)$$



such that applying equivariant monoid actions to  $E_i$  and  $V_i$  preserves the map  $v_i : E_i \rightarrow V_i$ . In general, the data fiber  $F_i$  cannot be assumed to be of the same type as the visual fiber  $P_i$  and the actions of  $M$  on  $F_i$  cannot be assumed to be the same as the actions of  $M'$  on  $P_i$ ; therefore an equivariant  $v_i$  must satisfy the constraint

$$v_i(m_r(E_i)) = \varphi(m_r)(v_i(E_i)) \quad (21)$$

such that  $\varphi$  maps a monoid action on data to a monoid action on visual elements. However, we can construct a monoid action of  $M$  on  $P_i$  that is compatible with a monoid action of  $M$  on  $F_i$ . We can compose the monoid actions on the visual fiber  $M' \times P_i \rightarrow P_i$  with the homomorphism  $\varphi$  that takes  $M$  to  $M'$ . This allows us to define a monoid action on  $P$  of  $M$  that is  $(m, v) \rightarrow \varphi(m) \bullet v$ . Therefore, without a loss of generality, we can assume that an action of  $M$  acts on  $F_i$  and on  $P_i$  compatibly such that  $\varphi$  is the identity function.

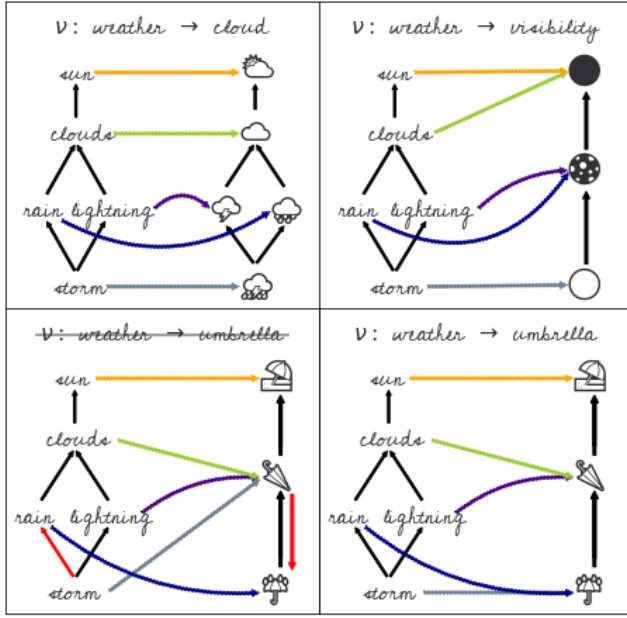


Fig. 6: Equivariant  $v$  maps the weather data to corresponding symbols such that the relative order of the symbols is the same as the data as shown in the top two panels. In the bottom right panel the ordering of *rain* and *storm* is swapped in the symbols, meaning that the  $v$  is invalid; in the bottom left panel, *storm* is instead mapped to the same symbol as *rain* so that the ordering is preserved.

scale	group	constraint
nominal	permutation	if $r_1 \neq r_2$ then $v(r_1) \neq v(r_2)$
ordinal	monotonic	if $r_1 \leq r_2$ then $v(r_1) \leq v(r_2)$
interval	translation	$v(x + c) = v(x) + c$
ratio	scaling	$v(xc) = v(x) * c$

The equivariance constraints for the Steven measurement scales [63] are derived from the mathematical group structure of the scales. For monoid actions, the equivariance constraint is that relative order is preserved, as shown in the top two panels of Fig. 6.

### 3.3.2 Visualization Assembly

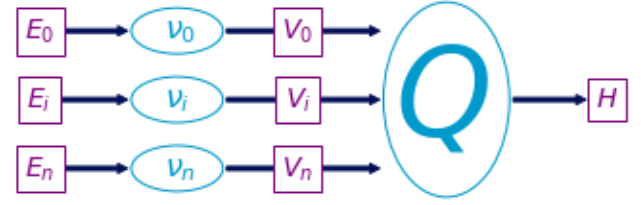


Fig. 7:  $v_i$  functions convert data  $\tau_i$  to visual characteristics  $\mu_i$ , then  $Q$  assembles  $\mu_i$  into a graphic  $\rho$  such that there is a map  $\xi$  preserving the continuity of the data.

As shown in Fig. 7,  $v$  and  $Q$  are analogous to a map-reduce operation: data components  $E_i$  are mapped into visual components  $V_i$  that are reduced into a graphic in  $H$ . The space of all graphics that  $Q$  can generate is the subset of graphics reachable via applying the reduction function  $Q(\Gamma(V)) \in \Gamma(H)$  to the visual section  $\mu \in \Gamma(V)$ . We formalize the expectation that visualization generation functions parameterized in the same way should generate the same functions as the equivariant map  $Q : \mu \mapsto \rho$ . We then define the constraint on  $Q$  such that if  $Q$  is applied to two visual sections  $\mu$  and  $\mu'$  that generate the same  $\rho$  then the output of  $\mu$  and  $\mu'$  acted on by the same monoid  $m$  must be the same. We cannot define monoid actions on all of  $\Gamma(H)$  because there are graphics  $\rho \in \Gamma(H)$  for which we cannot construct a valid mapping from  $V$ . Lets call the visual representations of the



Fig. 8: These two glyphs are generated by the same annulus  $Q$  function. The monoid action  $m_i$  on edge thickness  $\mu_i$  of the first glyph yields the thicker edge  $\mu_i'$  in the second glyph.

components  $\Gamma(V) = X$  and the graphic  $Q(\Gamma(V)) = Y$

**Proposition 1** If for elements of the monoid  $m \in M$  and for all  $\mu, \mu' \in X$ , we define the monoid action on  $X$  so that it is by definition equivariant

$$Q(\mu) = Q(\mu') \implies Q(m \circ \mu) = Q(m \circ \mu') \quad (22)$$

then a monoid action on  $Y$  can be defined as  $m \circ \rho = \rho'$ . If and only if  $Q$  satisfies Equation 22, we can state that the transformed graphic  $\rho' = Q(m \circ \mu)$  is equivariant to a monoid action applied on  $Q$  with input  $\mu \in Q^{-1}(\rho)$  that must generate valid  $\rho$ .

For example, given fiber  $P = (xpos, ypos, color, thickness)$ , then sections  $\mu = (0, 0, 0, 1)$  and  $Q(\mu) = \rho$  generates a piece of the thin hollow circle. The action  $m = (e, e, e, x + 2)$ , where  $e$  is identity, translates  $\mu$  to  $\mu' = (e, e, e, 3)$  and the corresponding action on  $\rho$  causes  $Q(\mu')$  to be the thicker circle in Fig. 8.

We formally describe a glyph as  $Q$  applied to the regions  $k$  that map back to a set of path connected components  $J \subset K$  as input

$$J = \{j \in K \text{ s. t. } \exists \gamma \text{ s.t. } \gamma(0) = k \text{ and } \gamma(1) = j\} \quad (23)$$

where the path [3]  $\gamma$  from  $k$  to  $j$  is a continuous function from the interval  $[0, 1]$ . We define the glyph as the graphic generated

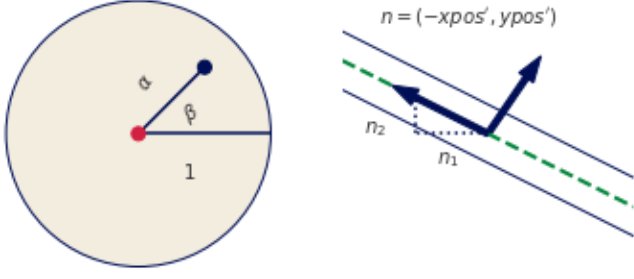


Fig. 9: The coordinates  $(\alpha, \beta)$  dictate the color of the region in prerender space  $S$  which over the whole disk generates the graphical mark. The line fiber is thickened with the derivative because the tangent the line needs to be pushed perpendicular to the tangent of  $(xpos, ypos)$  in order to have visible thickness.

by  $Q(S_j)$

$$H \xrightleftharpoons[\rho(S_j)]{\xi(s)} S_j \xrightleftharpoons[\xi^{-1}(j)]{\xi(s)} J_k \quad (24)$$

such that for every glyph there is at least one corresponding region on  $K$ , in keeping with the definition of glyph as any differentiable element put forth by Ziemkiewicz and Kosara [77]. The primitive point, line, and area marks [14, 23] are specially cased glyphs.

In Fig. 1, we illustrate the output of a minimal  $Q$  that will generate distinguishable graphical marks: non-overlapping scatter points, a non-infinitely thin line, and an image. The scatter plot can be defined as

$$Q(xpos, ypos)(\alpha, \beta) \quad (25)$$

where color  $\rho_{RGB} = (0, 0, 0)$  is defined as part of  $Q$  and  $s = (\alpha, \beta)$  defines the region on  $S$ . The position of this swatch of color can be computed relative to the location on the disc  $S_k$  as shown in Fig. 9

$$\begin{aligned} x &= \text{size} * \alpha \cos(\beta) + xpos \\ y &= \text{size} * \alpha \sin(\beta) + ypos \end{aligned}$$

such that  $\rho(s) = (x, y, 0, 0, 0)$  colors the point  $(x, y)$  black. In contrast, the line plot

$$Q(xpos, r1, ypos, r2)(\alpha, \beta) \quad (26)$$

in Fig. 1 has a  $\xi$  function that is not only parameterized on  $k$  but also on the  $\alpha$  distance along  $k$  and corresponding region in  $S$ . As shown in Fig. 9, line needs to know the tangent of the data to draw an envelope above and below each  $(xpos, ypos)$  such that the line appears to have a thickness; therefore the artist takes as input the jet bundle  $[4, 52] \mathcal{J}^2(E)$  which is the data  $E$  and the first and second derivatives of  $E$ . The magnitude of the slope is  $|n| = \sqrt{n_1^2 + n_2^2}$  such that the normal is  $r1 = \frac{n_1}{|n|}$ ,  $r2 = \frac{n_2}{|n|}$  which yields components of  $\rho$

$$\begin{aligned} x &= xpos(\xi(\alpha)) + \text{width} * \beta r1(\xi(\alpha)) \\ y &= ypos(\xi(\alpha)) + \text{width} * \beta r2(\xi(\alpha)) \end{aligned}$$

where  $(x, y)$  look up the position  $\xi(\alpha)$  on the data and the derivatives  $r1, r2$ . The derivatives are then multiplied by a width parameter to specify the thickness. In Fig. 1, the image

$$Q(xpos, ypos, color) \quad (27)$$

is a direct lookup into  $\xi: S \rightarrow K$ . The indexing variables  $(\alpha, \beta)$  define the distance along the space, which is then used by  $\xi$  to map into  $K$  to lookup the color values

$$R = R(\xi(\alpha, \beta)), G = G(\xi(\alpha, \beta)), B = B(\xi(\alpha, \beta))$$

In the case of an image, the indexing mapper  $\xi$  may do some translating to a convention expected by  $Q$ , for example reorienting the array such that the first row in the data is at the bottom of the graphic.

### 3.3.3 Assembly Factory

The graphic base space  $S$  is not accessible in many architectures, including Matplotlib; instead we can construct a factory function  $\hat{Q}$  over  $K$  that can build a  $Q$ . As shown in Equation 17,  $Q$  is a bundle map  $Q: \xi^*V \rightarrow H$  where  $\xi^*V$  and  $H$  are both bundles over  $S$ .

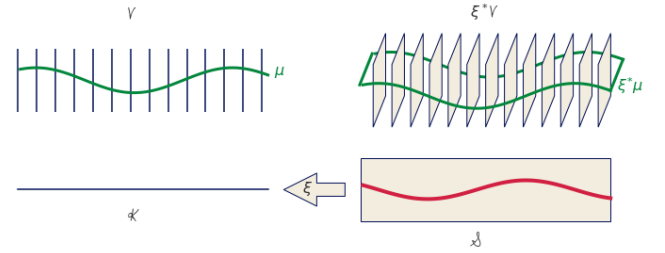


Fig. 10: Because the pullback of the visual bundle  $\xi^*V$  is the replication of a  $\mu$  over all points  $s$  that map back to a single  $k$ , we can construct a  $\hat{Q}$  on  $\mu$  over  $k$  that will fabricate the  $Q$  for the equivalent region of  $s$  associated to that  $k$

The preimage of the continuity map  $\xi^{-1}(k) \subset S$  is such that many graphic continuity points  $s \in S_k$  go to one data continuity point  $k$ ; therefore, by definition the pull back of  $\mu$

$$\xi^*V|_{\xi^{-1}(k)} = \xi^{-1}(k) \times P \quad (28)$$

copies the visual fiber  $P$  over the the points  $s$  in graphic space  $S$  that correspond to one  $k$  in data space  $K$ . This set of points  $s$  are the preimage  $\xi^{-1}(k)$  of  $k$ .

As shown in Fig. 10, given the section  $\xi^*\mu$  pulled back from  $\mu$  and the point  $s \in \xi^{-1}(k)$ , there is a direct map  $(k, \mu(k)) \mapsto (s, \xi^*\mu(s))$  from  $\mu$  over  $k$  to the section  $\xi^*\mu$  over  $s$ . This means that the pulled back section  $\xi^*\mu(s) = \xi^*(\mu(k))$  is the section  $\mu$  copied over all  $s$  such that  $\xi^*\mu$  is identical for all  $s$  where  $\xi(s) = k$ . In Fig. 10 each dot on  $P$  is equivalent to the line on  $P^*\mu$ .

Given the equivalence between  $\mu$  and  $\xi^*\mu$  defined above, the reliance on  $S$  can be factored out. When  $Q$  maps visual sections into graphics  $Q: \Gamma(\xi^*V) \rightarrow \Gamma(H)$ , if we restrict  $Q$  input to  $\xi^*\mu$  then the graphic section  $\rho$  evaluated on a visual region  $s$

$$\rho(s) := Q(\xi^*\mu)(s) \quad (29)$$

is defined as the assembly function  $Q$  with input  $\xi^*\mu$  evaluated on  $s$ . Since the pulled back section  $\xi^*\mu$  is the section  $\mu$  copied over every graphic region  $s \in \xi^{-1}(k)$ , we can define a  $Q$  factory function

$$\hat{Q}(\mu(k))(s) := Q((\xi^*\mu)(s)) \quad (30)$$

where  $\hat{Q}$  with input  $\mu$  is defined to  $Q$  that takes as input the copied section  $\xi^*\mu$  such that both functions are evaluated over the same location  $\xi^{-1}(k) = s$  in the base space  $S$ . Factoring out  $s$  from Equation 30 yields

$$\hat{Q}(\mu(k)) = Q(\xi^*\mu) \quad (31)$$

where  $Q$  is no longer bound to input but  $\hat{Q}$  is still defined in terms of  $K$ . In fact,  $\hat{Q}$  is a map from visual space to graphic space<sup>1</sup>  $\hat{Q} : \Gamma(V) \rightarrow \Gamma(H)$  locally over  $k$  such that it can be evaluated on<sup>2</sup> a single visual record  $\hat{Q} : \Gamma(V_k) \rightarrow \Gamma(H|_{\xi^{-1}(k)})$ . This allows us<sup>3</sup> to construct a  $\hat{Q}$  that only depends on  $K$ , such that for each  $\mu(k)$ <sup>4</sup> there is part of  $\rho|_{\xi^{-1}(k)}$ . The construction of  $\hat{Q}$  allows us to<sup>5</sup> retain the functional map reduce benefits of  $Q$  without having to<sup>6</sup> majorly restructure the existing pipeline for libraries that delegate<sup>7</sup> the construction of  $\rho$  to a back end such as Matplotlib.<sup>8</sup>

### 3.3.4 Composite and Reusable Artists

Given the family of artists ( $E_i : i \in I$ ) on the same image, the + operator

$$+ := \bigsqcup_{i \in I} E_i \quad (32)$$

defines a simple composition of artists. When artists share a base space  $K_2 \hookrightarrow K_1$ , a composition operator can be defined such that the artists are acting on different components of the same section. This type of composition is important for visualizations where elements update together in a consistent way, such as multiple views [9, 55] and brush-linked views [13, 18]. It is impractical to implement an artist for every single graphic; instead we implement an approximation of the equivalence class of artists

$$\{A \in A' : A_1 \equiv A_2\} \quad (33)$$

Roughly, two artists are equivalent if they have the same visual fiber  $P$  assembly function  $Q$  and continuity map  $\xi$ .

## 4 PROTOTYPE

To build a prototype, we make use of the Matplotlib figure and axes artists [42, 43] so that we can initially focus on the data to graphic transformations and exploit the Matplotlib transform stack to transform data coordinates into screen coordinates. While the artist is specified in a fully functional manner in Equation 17, we implement our prototype in a heavily object oriented manner. This is a concession to existing Matplotlib architecture and so that the object can do bookkeeping of parameter information. But, in keeping with functional norms, we attempt to pass around as little information as necessary.

```
1 fig, ax = plt.subplots()
2 artist = Artist(data, transforms)
3 ax.add_artist(artist)
```

Building on the current Matplotlib artists which construct an internal representation of the graphic, `ArtistClass` acts as an equivalence class artist  $A'$  as described in Equation 33. The visual bundle  $V$  is specified as the transform dictionary of the form  $\{\text{parameter} : (\text{variable}, \text{encoder})\}$  where `parameter` is a component in  $P$ , `variable` is a component in  $F$ , and the  $v$  encoders are passed in as functions or callable objects. The data bundle  $E$  is passed in as a data object. By binding data and transforms to  $A'$  inside `__init__`, the `draw` method is a fully specified artist  $A$  as defined in Equation 15.

```
1 class ArtistClass(matplotlib.artist.Artist): #A'
2     def __init__(self, data, transforms, *args, **kwargs):
3         # properties that are specific to the graphic
4         self.data = data #E
5         self.transforms = transforms #V
6         super().__init__(*args, **kwargs)
7
8     def assemble(self, **args): #\hat{Q}
9         # set the properties of the graphic
```

```
def draw(self, renderer): #A
    # returns K, indexed on fiber then key
    view = self.data.view(self.axes) #\tau
    # visual channel encoding applied fiberwise
    # \nu_i(\tau_i)
    visual = {p: t['encoder'](view[t['name']])
              for p, t in self.transforms.items()}
    self.assemble(**visual)
    # pass configurations off to the renderer
    super().draw(renderer)
```

The data is fetched in section  $\tau$  via a `view` method on the data because the input to the artist is a section on  $E$ . The `view` method takes the axes attribute because it provides the region in graphic coordinates  $S$  that can be used to query back into data to select a subset. To ensure the integrity of the section, `view` must be atomic, which means that the values cannot change after the method is called in `draw` until a new call in `draw`. We put this constraint on the return of the `view` method so that we do not risk race conditions.

The  $v$  functions are then applied to the data, as describe in Equation 19, to generate the visual section  $\mu$  that here is the object `visual`. The conversion from data to visual space is simplified here to directly show that it is the encoding  $v$  applied to the component. The `assemble` function that is  $\hat{Q}$ , as defined in Equation 31, is responsible for generating a representation such that it could be serialized to recreate a static version of the graphic. This artist is not optimized because we prioritized demonstrating the separability of  $v$  and  $\hat{Q}$ . The last step in the artist function is handing itself off to the renderer. The extra `*arg`, `**kwargs` arguments in `__init__`, `draw` are artifacts of how these objects are currently implemented.

### 4.1 Scatter and Line Artists

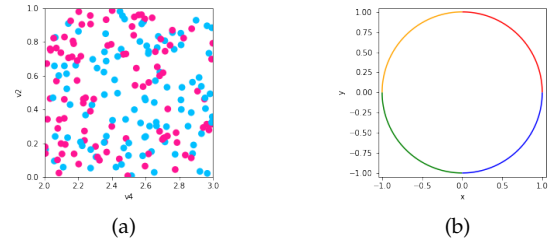


Fig. 11: Scatter plot and line plot implemented using prototype artists and data models, building on Matplotlib rendering.

To generate the figure in Fig. 11a, the `Point` artist builds on collection artists because collections are optimized to efficiently draw a sequence of primitive point and area marks. In this prototype, the scatter marker shape is fixed as a circle, and the only visual fiber components are  $x$  and  $y$  position, size, and the facecolor of the marker, as described by Equation 25. We only show the `assemble` function here because the `__init__`, `draw` are identical the prototype artist. The `view` method repackages the data as a fiber component indexed table of vertices. Even though the `view` is fiber indexed, each vertex at an index  $k$  has corresponding values in section  $\tau(k_i)$ . This means that all the data on one vertex maps to one glyph.

```
1 class Point(mcollections.Collection):
2     def assemble(self, x, y, s, facecolors='C0'): #\hat{Q}
3         # construct geometries of circle glyphs
```

```

4     self._paths = [mpath.Path.circle((xi,yi), radius=si)
5                     for (xi, yi, si) in zip(x, y, s)]
6     # set attributes of glyphs, these are vectorized
7     # circles and facecolors are lists of the same size
8     self.set_facecolors(facecolors)

```

```

1 @dataclass
2 class FiberBundle:
3     K: dict #{'tables': []}
4     F: dict # {variable name: type}

```

In assemble, the  $\mu$  components are used to construct the vector path of each circular marker with center (x,y) and size x and set the colors of each circle. This is done via the Path.circle object.

```

1 class Line(mcollections.LineCollection):
2     def assemble(self, x, y, color='C0'): #\hat{Q}
3         #assemble line marks as set of segments
4         segments = [np.vstack((vx, vy)).T for vx, vy
5                       in zip(x, y)]
6         self.set_segments(segments)
7         self.set_color(color)

```

that asks the user to specify the the properties of F and the K connectivity in terms of a simplicial triangulation scheme [31]. To generate the scatter plot and the line plot, the distinction is in the tau method that is the section.

```

1 class VertexSimplex:
2     """Fiberbundle is consistent across all sections
3     """
4     FB = FiberBundle({'tables': ['vertex']},
5                      {'v1': float, 'v2': str, 'v3': float})
6
7     def __init__(self, sid = 45, size=1000, max_key=10**10):
8         # create random list of keys
9     def tau(self, k):
10        # e1 is sampled from F1, e2 from F2, etc...
11        return (k, (e1, e2, e3, e4))

```

To generate Fig. 11b, the Line artist view method returns a table of edges. Each edge consists of (x,y) points sampled along the edge, defined by the edge and information such as the color of the edge. As with Point, the data is then converted into visual variables. In assemble, described by Equation 26, this visual representation is composed into a set of line segments, where each segment is the array generated by np.vstack((vx, vy)). Then the colors of each line segment are set. The colors are guaranteed to correspond to the correct segment because of the atomicity constraint on view.

The discrete tau method returns a record of discrete points, while the linetau returns a sampling of points along an edge k

#### 4.1.1 Visual Encoders

The visual parameter serves as the dictionary key because the visual representation is constructed from the encoding applied to the data  $\mu = \nu \circ \tau$ . For the scatter plot, the mappings for the visual fiber components  $P = (x, y, \text{facecolors}, s)$  are defined as

```

1 def tau(self, k): #will fix location on page on revision
2     x, y = self._xy(k, self.distances,
3                     self.angle_samples[k], self.angle_samples[k+1])
4     color = self._color(k)
5     return (k, (x, y, color))

```

```

1 cmap = color.Categorical({'true': 'deeppink',
2                           'false': 'deepskyblue'})
3 # {P_i name:{'name':c_i, 'encoder':\nu_i}}
4 transforms = {'x': {'name': 'v4', 'encoder': lambda x: x},
5               'y': {'name': 'v2', 'encoder': lambda x: x},
6               'facecolors': {'name': 'v3', 'encoder': cmap},
7               's': {'name': None,
8                    'encoder': lambda _: itertools.repeat(.02)}}

```

In both cases the view method packages the data

```

1 def view(self, axes):
2     table = defaultdict(list)
3     for k in self.keys:
4         table['index'].append(k)
5         for (name, value) in zip(self.FB.fiber.keys(),
6                                 self.tau(k)[1]):
7             table[name].append(value)
8     return table

```

where  $\lambda x: x$  is an identity  $\nu$ ,  $\{\text{'name':None}\}$  maps into  $P$  without corresponding  $\tau$  to set a constant visual value, and color.Categorical is a custom  $\nu$  implemented as a class for reusability. A test for equivariance, as described in Equation 21, can be implemented trivially

into a data structure that the artist can unpack via data component name.

```

1 #\nu_i(m_r(E_i)) = \varphi(m_r)(\nu_i(E_i))
2 def test_nominal(values, encoder):
3     m1 = list(zip(values, encoder(values)))
4     random.shuffle(values)
5     m2 = list(zip(values, encoder(values)))
6     assert sorted(m1) == sorted(m2)

```

but is currently factored out of the artist for clarity.

#### 4.1.2 Data Model

The data input into the Artist will often be a wrapper class around an existing data structure. This wrapper object must specify the fiber components F and connectivity K and have a view method that returns an atomic object that encapsulates  $\tau$ . To support specifying the fiber bundle, we define a FiberBundle data class [1]

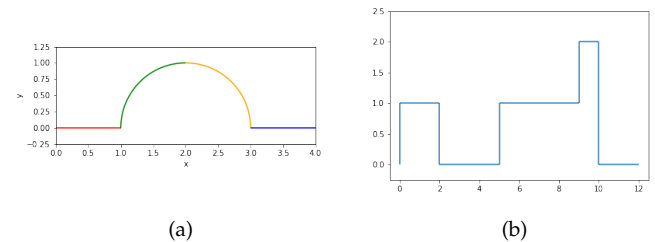


Fig. 12: Continuous and discontinuous lines as defined via the same data model, and generated with the same A'Line

The graphics in figure Fig. 12 are made using the Line artist and the Graphline data source where if told that the data is connected,



the data source will check for that connectivity by constructing an adjacency matrix. The multicolored line is a connected graph of edges with each edge function evaluated on 1000 samples,

```
1 simplex.GraphLine(FB, edges, verticies,  
2                     num_samples=1000, connect=True)
```

while the stair chart is discontinuous and only needs to be evaluated at the edges of the interval

```
1 simplex.GraphLine(FB, edges, verticies,  
2                     num_samples=2, connect=False)
```

such that one advantage of this model is it helps differentiate graphics that have different artists from graphics that have the same artist but make different assumptions about the source data.

## 5 Discussion

This work contributes a mathematical description of the mapping  $A$  from data to visual representation. Combining Butler’s proposal of a fiber bundle model of visualization data with Spivak’s formalism of schema lets this model support a variety of datasets, including discrete relational tables,, multivariate high resolution spatio temporal datasets, and complex networks. Decomposing the artist into encoding  $v$ , assembly  $Q$ , and reindexing  $\xi$ , provides the specifications that the graphic must have continuity equivalent to the data, and that the visual characteristics of the graphics are equivariant to their corresponding components under monoid actions. This model defines these constraints on the transformation function such that they are not specific to any one type of encoding or visual characteristic. Encoding the graphic space as a fiber bundle provides a structure rich abstraction of the target graphical design in the target display space. The toy prototype built using this model validates that is usable for a general purpose visualization tool since it can be iteratively integrated into the existing architecture rather than starting from scratch. Factoring out graphic formation into assembly functions allows for much more clarity in how they differ. This prototype demonstrates that this framework can generate the fundamental point (scatter plot) and line (line chart) marks.

### 5.1 Limitations

So far this model has only been worked out for a single data set tied to a primitive mark. The examples and prototype have so far only been implemented for the static 2D case, but nothing in the math limits to 2D and expansion to the animated case should be possible because the model is formalized in terms of the sheaf. While this model supports equivariance of figurative glyphs generated from parameters of the data [12,22], it does not have a way to evaluate the semantic accuracy of the figurative representation. Even though the model is designed to be backend and format independent, it has only really been tested against PNGs rendered with the AGG backend. It is especially unknown how this framework interfaces with high performance rendering libraries such as OpenGL [24]. This model and the associated prototype is deeply tied to Matplotlib’s existing architecture, so it has not been worked through how the model generalizes to other libraries, such as those built on Mackinlay’s APT framework.

### 5.2 Future Work

More work is needed to formalize the composition operators and equivalence class  $A'$ . More artists need to be implemented to demonstrate that the model can underpin a minimally viable library, foremost an image [35,38,68], a heatmap [46,74], and an

inherently computational artist such as the boxplot [72]. This could be pushed further to integrate with topological [41] and functional [56] data analysis methods. Since this model formalizes notions of structure preservation, it can serve as a good base for tools that assess quality metrics [15] or invariance [44] of visualizations with respect to graphical encoding choices. While this paper formulates visualization in terms of monoidal action homomorphisms between fiberbundles, the model lends itself to a categorical formulation [29,50] that could be further explored.

## 6 Conclusion

An unofficial philosophy of Matplotlib is to support making whatever kinds of plots a user may want, even if they seem nonsensical to the development team. The topological framework described in this work provides a way to facilitate this graph creation in a rigorous manner; any artist that meets the equivariance criteria described in this work by definition generates a graphic representation that matches the structure of the data being represented. We leave it to domain specialists to define the structure they need to preserve and the maps they want to make, and hopefully make the process easier by untangling these components into separate constrained maps and providing a fairly general data and display model.

## Acknowledgments

The authors wish to thank the Matplotlib development team for their invaluable feedback along the way, particularly Bruno Beltran. This project has been made possible in part by grant number 2019-207333 from the Chan Zuckerberg Initiative DAF, an advised fund of Silicon Valley Community Foundation.

## References

- [1] Dataclasses — Data Classes — Python 3.9.2rc1 documentation. <https://docs.python.org/3/library/dataclasses.html>.
- [2] Locally trivial fibre bundle - Encyclopedia of Mathematics. [https://encyclopediaofmath.org/wiki/Locally\\_trivial\\_fibre\\_bundle](https://encyclopediaofmath.org/wiki/Locally_trivial_fibre_bundle).
- [3] Connected space. *Wikipedia*, Dec. 2020.
- [4] Jet bundle. *Wikipedia*, Dec. 2020.
- [5] Quotient space (topology). *Wikipedia*, Nov. 2020.
- [6] Retraction (topology). *Wikipedia*, July 2020.
- [7] Monoid. *Wikipedia*, Jan. 2021.
- [8] Semigroup action. *Wikipedia*, Jan. 2021.
- [9] Y. Albo, J. Lanir, P. Bak, and S. Rafaeli. Off the Radar: Comparative Evaluation of Radial Visualization Solutions for Composite Indicators. *IEEE Transactions on Visualization and Computer Graphics*, 22(1):569–578, Jan. 2016. doi: 10.1109/TVCG.2015.2467322
- [10] P. D. Auroux. Math 131: Introduction to Topology. p. 113.
- [11] M. Bastian, S. Heymann, and M. Jacomy. Gephi: An Open Source Software for Exploring and Manipulating Networks. *Proceedings of the International AAAI Conference on Web and Social Media*, 3(1), Mar. 2009.
- [12] F. Beck. Software Feathers figurative visualization of software metrics. In *2014 International Conference on Information Visualization Theory and Applications (IVAPP)*, pp. 5–16, Jan. 2014.
- [13] R. A. Becker and W. S. Cleveland. Brushing Scatterplots. *Technometrics*, 29(2):127–142, May 1987. doi: 10.1080/00401706.1987.10488204
- [14] J. Bertin. *Semiology of Graphics : Diagrams, Networks, Maps*. ESRI Press, Redlands, Calif., 2011.
- [15] E. Bertini, A. Tatu, and D. Keim. Quality metrics in high-dimensional data visualization: An overview and systematization. *IEEE Transactions on Visualization and Computer Graphics*, 17(12):2203–2212, 2011.
- [16] M. Bostock, V. Ogievetsky, and J. Heer. D<sup>3</sup> Data-Driven Documents. *IEEE Transactions on Visualization and Computer Graphics*, 17(12):2301–2309, Dec. 2011. doi: 10.1109/TVCG.2011.185
- [17] R. Brüggemann and G. P. Patil. *Ranking and Prioritization for Multi-Indicator Systems: Introduction to Partial Order Applications*. Springer Science & Business Media, July 2011.
- [18] A. Buja, J. A. McDonald, J. Michalak, and W. Stuetzle. Interactive data visualization using focusing and linking. In *Proceedings of*

- the 2nd Conference on Visualization '91, VIS '91, pp. 156–163. IEEE Computer Society Press, Washington, DC, USA, 1991.
- [19] D. M. Butler and S. Bryson. Vector-Bundle Classes form Powerful Tool for Scientific Visualization. *Computers in Physics*, 6(6):576, 1992. doi: 10.1063/1.4823118
- [20] D. M. Butler and M. H. Pendley. A visualization model based on the mathematics of fiber bundles. *Computers in Physics*, 3(5):45, 1989. doi: 10.1063/1.168345
- [21] L. Byrne, D. Angus, and J. Wiles. Acquired Codes of Meaning in Data Visualization and Infographics: Beyond Perceptual Primitives. *IEEE Transactions on Visualization and Computer Graphics*, 22(1):509–518, Jan. 2016. doi: 10.1109/TVCG.2015.2467321
- [22] L. Byrne, D. Angus, and J. Wiles. Figurative frames: A critical vocabulary for images in information visualization. *Information Visualization*, 18(1):45–67, Aug. 2017. doi: 10.1177/1473871617724212
- [23] S. Carpendale. Visual Representation from Semiology of Graphics by J. Bertin.
- [24] G. S. Carson. Standards pipeline: The OpenGL specification. *SIG-GRAPH Comput. Graph.*, 31(2):17–18, May 1997. doi: 10.1145/271283.271292
- [25] A. M. Cegarra. Cohomology of monoids with operators. In *Semi-group Forum*, vol. 99, pp. 67–105. Springer, 2019.
- [26] C.-S. J. Chu. Time series segmentation: A sliding window approach. *Information Sciences*, 85(1):147–173, July 1995. doi: 10.1016/0020-0255(95)00021-G
- [27] M. S. Crouch, A. McGregor, and D. Stubbs. Dynamic graphs in the sliding-window model. In *European Symposium on Algorithms*, pp. 337–348. Springer, 2013.
- [28] J. Ellson, E. Gansner, L. Koutsofios, S. C. North, and G. Woodhull. Graphviz—Open Source Graph Drawing Tools. In P. Mutzel, M. Jünger, and S. Leipert, eds., *Graph Drawing*, pp. 483–484. Springer Berlin Heidelberg, Berlin, Heidelberg, 2002.
- [29] B. Fong and D. I. Spivak. *An Invitation to Applied Category Theory: Seven Sketches in Compositionality*. Cambridge University Press, first ed., July 2019. doi: 10.1017/9781108668804
- [30] M. Friendly. *A Brief History of Data Visualization*, pp. 15–56. Springer Berlin Heidelberg, Berlin, Heidelberg, 2008. doi: 10.1007/978-3-540-33037-0\_2
- [31] J.-D. B. Geometria. Simplicial Complexes. p. 52.
- [32] B. Geveci, W. Schroeder, A. Brown, and G. Wilson. VTK. *The Architecture of Open Source Applications*, 1:387–402, 2012.
- [33] R. Ghrist. Homological algebra and data. *Math. Data*, 25:273, 2018.
- [34] R. W. Ghrist. *Elementary Applied Topology*, vol. 1. Createspace Seattle, 2014.
- [35] R. B. Haber and D. A. McNabb. Visualization idioms: A conceptual model for scientific visualization systems. *Visualization in scientific computing*, 74:93, 1990.
- [36] A. Hagberg, D. A. Schult, and P. J. Swart. Exploring network structure, dynamics, and function using NetworkX. In G. Varoquaux, T. Vaught, and J. Millman, eds., *Proceedings of the 7th Python in Science Conference*, pp. 11–15. Pasadena, CA USA, 2008.
- [37] P. Hanrahan. VizQL: A language for query, analysis and visualization. In *Proceedings of the 2006 ACM SIGMOD International Conference on Management of Data, SIGMOD '06*, p. 721. Association for Computing Machinery, New York, NY, USA, 2006. doi: 10.1145/1142473.1142560
- [38] C. D. Hansen and C. R. Johnson. *Visualization Handbook*. Elsevier, 2011.
- [39] M. D. Hanwell, K. M. Martin, A. Chaudhary, and L. S. Avila. The Visualization Toolkit (VTK): Rewriting the rendering code for modern graphics cards. *SoftwareX*, 1-2:9–12, Sept. 2015. doi: 10.1016/j.softx.2015.04.001
- [40] J. Heer and M. Agrawala. Software design patterns for information visualization. *IEEE Transactions on Visualization and Computer Graphics*, 12(5):853–860, 2006. doi: 10.1109/TVCG.2006.178
- [41] C. Heine, H. Leitte, M. Hlawitschka, F. Iurich, L. De Floriani, G. Scheuermann, H. Hagen, and C. Garth. A Survey of Topology-based Methods in Visualization. *Computer Graphics Forum*, 35(3):643–667, June 2016. doi: 10.1111/cgf.12933
- [42] J. Hunter and M. Droettboom. The Architecture of Open Source Applications (Volume 2): Matplotlib. <https://www.aosabook.org/en/matplotlib.html>.
- [43] J. D. Hunter. Matplotlib: A 2D graphics environment. *Computing in Science Engineering*, 9(3):90–95, May 2007. doi: 10.1109/MCSE.2007.55
- [44] G. Kindlmann and C. Scheidegger. An Algebraic Process for Visualization Design. *IEEE Transactions on Visualization and Computer Graphics*, 20(12):2181–2190, Dec. 2014. doi: 10.1109/TVCG.2014.2346325
- [45] W. A. Lea. A formalization of measurement scale forms. p. 44.
- [46] T. Loua. *Atlas Statistique de La Population de Paris*. J. Dejeu & cie, 1873.
- [47] J. Mackinlay. Automating the design of graphical presentations of relational information. *ACM Transactions on Graphics*, 5(2):110–141, Apr. 1986. doi: 10.1145/22949.22950
- [48] J. Mackinlay. *Automatic Design of Graphical Presentations*. PhD Thesis, Stanford, 1987.
- [49] J. Mackinlay, P. Hanrahan, and C. Stolte. Show me: Automatic presentation for visual analysis. *IEEE Transactions on Visualization and Computer Graphics*, 13(6):1137–1144, Nov. 2007. doi: 10.1109/TVCG.2007.70594
- [50] B. Milewski. Category Theory for Programmers. p. 498.
- [51] T. Munzner. *Visualization Analysis and Design*. AK Peters Visualization Series. CRC press, Oct. 2014.
- [52] J. Musilová and S. Hronek. The calculus of variations on jet bundles as a universal approach for a variational formulation of fundamental physical theories. *Communications in Mathematics*, 24(2):173–193, Dec. 2016. doi: 10.1515/cm-2016-0012
- [53] D. Nekrasovski, A. Bodnar, J. McGrenere, F. Guimbretière, and T. Munzner. An evaluation of pan & zoom and rubber sheet navigation with and without an overview. In *Proceedings of the SIGCHI Conference on Human Factors in Computing Systems, CHI '06*, pp. 11–20. Association for Computing Machinery, New York, NY, USA, 2006. doi: 10.1145/1124772.1124775
- [54] nLab authors. Action. Mar. 2021.
- [55] Z. Qu and J. Hullman. Keeping multiple views consistent: Constraints, validations, and exceptions in visualization authoring. *IEEE Transactions on Visualization and Computer Graphics*, 24(1):468–477, Jan. 2018. doi: 10.1109/TVCG.2017.2744198
- [56] J. O. Ramsay. *Functional Data Analysis*. Wiley Online Library, 2006.
- [57] A. Satyanarayan, K. Wongsuphasawat, and J. Heer. Declarative interaction design for data visualization. In *Proceedings of the 27th Annual ACM Symposium on User Interface Software and Technology*, pp. 669–678. ACM, Honolulu Hawaii USA, Oct. 2014. doi: 10.1145/2642918.2647360
- [58] C. A. Schneider, W. S. Rasband, and K. W. Eliceiri. NIH Image to ImageJ: 25 years of image analysis. *Nature Methods*, 9(7):671–675, July 2012. doi: 10.1038/nmeth.2089
- [59] N. Sofroniew, T. Lambert, K. Evans, P. Winston, J. Nunez-Iglesias, G. Bokota, K. Yamauchi, A. C. Solak, ziyangczi, G. Buckley, M. Bussonnier, D. D. Pop, T. Tung, V. Hilsenstein, Hector, J. Freeman, P. Boone, alisterburt, A. R. Lowe, C. Gohlke, L. Royer, H. Har-Gil, M. Kittisopikul, S. Axelrod, kir0ul, A. Patil, A. McGovern, A. Rokem, Bryant, and G. Peña-Castellanos. Napari/napari: 0.4.5rc1. Zenodo, Feb. 2021. doi: 10.5281/zenodo.4533308
- [60] E. Spanier. *Algebraic Topology*. McGraw-Hill Series in Higher Mathematics. Springer, 1989.
- [61] D. I. Spivak. SIMPLICIAL DATABASES. p. 35.
- [62] D. I. Spivak. Databases are categories, June 2010.
- [63] S. S. Stevens. On the Theory of Scales of Measurement. *Science*, 103(2684):677–680, 1946.
- [64] M. Stieven. A Monad is just a Monoid... <https://medium.com/@michelestieven/a-monad-is-just-a-monoid-a02bd2524f66>, Apr. 2020.
- [65] C. Stolte, D. Tang, and P. Hanrahan. Polaris: A system for query, analysis, and visualization of multidimensional relational databases. *IEEE Transactions on Visualization and Computer Graphics*, 8(1):52–65, Jan. 2002. doi: 10.1109/2945.981851
- [66] S. Studies. Culturevis/imageplot, Jan. 2021.
- [67] T. Sugibuchi, N. Spyrtatos, and E. Siminenko. A framework to analyze information visualization based on the functional data model. In *2009 13th International Conference Information Visualisation*, pp. 18–24, 2009. doi: 10.1109/IV.2009.56
- [68] M. Tory and T. Moller. Rethinking visualization: A high-level taxonomy. In *IEEE Symposium on Information Visualization*, pp. 151–158, 2004. doi: 10.1109/INFVIS.2004.59

- 742 [69] D. Urbanik. A Brief Introduction to Schemes and Sheaves. p. 16.
- 743 [70] J. VanderPlas, B. Granger, J. Heer, D. Moritz, K. Wongsuphasawat,
- 744 A. Satyanarayan, E. Lees, I. Timofeev, B. Welsh, and S. Sievert.
- 745 Altair: Interactive Statistical Visualizations for Python. *Journal of*
- 746 *Open Source Software*, 3(32):1057, Dec. 2018. doi: 10.21105/joss.01057
- 747 [71] H. Wickham. *Ggplot2: Elegant Graphics for Data Analysis*. Springer-
- 748 Verlag New York, 2016.
- 749 [72] H. Wickham and L. Stryjewski. 40 years of boxplots. *The American*
- 750 *Statistician*, 2011.
- 751 [73] L. Wilkinson. *The Grammar of Graphics*. Statistics and Computing.
- 752 Springer-Verlag New York, Inc., New York, 2nd ed ed., 2005.
- 753 [74] L. Wilkinson and M. Friendly. The History of the Cluster Heat Map.
- 754 *The American Statistician*, 63(2):179–184, May 2009. doi: 10.1198/tas.
- 755 2009.0033
- 756 [75] K. Wongsuphasawat. Navigating the Wide World of Data Visual-
- 757 ization Libraries (on the web), 2021.
- 758 [76] B. A. Yorgey. Monoids: Theme and Variations (Functional Pearl).
- 759 p. 12.
- 760 [77] C. Ziemkiewicz and R. Kosara. Embedding Information Visualiza-
- 761 tion within Visual Representation. In Z. W. Ras and W. Ribarsky,
- 762 eds., *Advances in Information and Intelligent Systems*, pp. 307–326.
- 763 Springer Berlin Heidelberg, Berlin, Heidelberg, 2009. doi: 10.1007/
- 764 978-3-642-04141-9\_15